Thin Solid Films 519 (2011) 6649–6653

Contents lists available at ScienceDirect

Thin Solid Films

journal homepage: www.elsevier.com/locate/tsf

The effect of the magnetron sputtering gun size on the characteristics of the plasma and CN_x film deposition

Ki-Min Roh [a], Shin-Jae You [b], Dae-Woong Kim [c], Jun-Hee Han [b], Jung-Hyung Kim [b,*], Dae-Jin Seong [b]

[a] Mineral Resource Research division, Korea Institute of Geoscience and Mineral Resources, Daejeon, 305-350, Republic of Korea
[b] Center for Vacuum Technology, Korea Research Institute of Standards and Science, Daejeon, 305-340, Republic of Korea
[c] Department of Physics, KAIST, Daejeon, 305-701, Republic of Korea

ARTICLE INFO

Available online 22 April 2011

Keywords:
Carbon nitride
Fourier transform infrared spectroscopy (FTIR)
Indentation
Null point
Sputtering gun

ABSTRACT

To investigate the effect of the gun size on plasma and carbon nitride film deposition characteristics in RF magnetron sputtering system, we performed the RF sputtering deposition with different gun sizes and targets (50.8 mm and 76.2 mm in diameter). The result shows that there are remarkable different results between two magnetron sputtering guns: in plasma measurement result, the 50.8 mm gun made a column-like discharge from the target to substrate where the deposition takes place, but the 76.2 mm gun made a small volume discharge confined nearby the target, in FTIR spectra and hardness test result, the CN_x films deposited by the 50.8 mm gun contained more sp^3 C – N bonds, and less hydrogenated bonds and better nano-hardness, compared with those by the 76.2 mm gun. This result is ascribed to the fact that the magnetic field configuration evolution, especially the null point difference, with varying gun size can influence the plasma structure and film property changes.

1. Introduction

Several decade years ago, Liu and Cohen theoretically predicted the structural and physical properties of β-C_3N_4 of which bulk modulus and hardness are comparable to or even greater than those of diamond [1]. Although the extensive studies have been carried out to synthesize this new material [2–8], in most cases, amorphous carbon nitride films instead of crystalline β-C_3N_4 were obtained and no group has reported the product of perfect crystalline films so far. However, after being known that amorphous carbon nitride also possesses attractive and potentially useful mechanical properties, such as high hardness and low friction coefficient [9–11], CN_x films have received much attention.

Among the variety of techniques to synthesize CN_x films such as the magnetron sputtering, laser ablation, ion beam deposition, and chemical vapor deposition (CVD), magnetron sputtering is one of the preferred methods because of its effective dissociation of nitrogen molecule, simple scalability and easy control of deposition conditions [12,13]. However, the insufficient numbers of sp^3 carbon and hydrogen-termination structures in CN_x films deposited by the magnetron sputtering method remain problems of synthesizing wear-resistance films [14]. In order to solve these problems, most of the studies have focused on the evolution of plasma and material properties only in terms of internal process parameters, such as substrate temperature, substrate bias voltage, and gas pressure [14,15], however, the influence of processing equipment, especially the sputtering gun, on the film characteristics has been undervalued. Although the diverse subjects related with the sputtering gun, such as application for the large area film depositions [16], effects of balanced/unbalanced magnetron guns [17,18], and deposition characteristics with different targets [19] had been studied, the influence of the gun size on the ion energy has not been investigated so far.

In this paper, we deposited CN_x films using different guns 50.8 and 76.2 mm (2 and 3 in.) in diameter to investigate the effect of the gun size on plasma and film characteristics. The microstructure and mechanical properties of carbon nitride films were analyzed by Fourier transform infrared spectroscopy (FTIR) and nano-indentation test. In experimental result, the CN_x films deposited by the 50.8 mm gun contained more sp^3 C – N bonds, and less hydrogenated bonds and better nano-hardness, compared with those by the 76.2 mm gun. From computer simulation technology electromagnetic (CST EM) studio simulation of magnetic field line configurations around the gun surface, we revealed that there were remarkable different positions of the magnetic null point between two magnetron sputtering guns. The influence of the null point change with varying gun size on the plasma structure and film property changes was also discussed.

2. Experiment

Deposition of CN_x films on single crystalline Si (100) was carried out using a radio frequency (RF) magnetron sputtering system. The experiments were performed at a pressure of 0.27–4.00 Pa with pure

* Corresponding author. Tel.: +82 42 868 5644; fax: +82 42 868 5285.
E-mail address: jhkim86@kriss.re.kr (J.-H. Kim).

0040-6090/$ – see front matter © 2011 Elsevier B.V. All rights reserved.
doi:10.1016/j.tsf.2011.04.089

N_2 (99.9999% purity). Carbon was sputtered from high-purity (99.995%) graphite targets, 50.8 and 76.2 mm in diameters positioned 10 cm from the substrate. The 50.8 mm target thickness was 3.2 mm and the 76.2 mm target thickness was 6.4 mm. The average target power during sputtering was 150 W. All CN_x films were deposited with the thickness of 600 nm.

CST EM Studio [20] was used for a calculation of magnetic field line configuration and phase change by the 50.8 and 76.2 mm magnetron sputtering guns. The geometrical details and cross section view of the guns were shown in Fig. 1. The body of the gun was made of copper and magnetic yoke on the bottom of the magnets was made of iron. A magnet 10 mm in diameter was positioned at the center of the gun and 12 magnets were arranged in a circle at the edge of the guns. The magnetic field intensity on the surface of each magnet was 0.1 T. The distances from the center to the side magnet in the 50.8 and 76.2 mm guns were respectively 25.4 and 38.1 mm. We could find the location of magnetic null point, intensity and flux of magnetic field around the sputtering gun by this simulator.

The composition and chemical structure of the CN_x films were analyzed using FTIR [14]. Transmission FTIR spectra were obtained using a Thermo Nicolet 360 spectrometer equipped with a KBr interferometer over a range of 650–4000 cm^{-1}. The background spectrum was independently measured on a pure silicon substrate. The spectra were recorded at a resolution of 4 cm^{-1} after being averaged over 32 scans per sample.

Nano Indenter II of Nano Instruments, Inc. was used for the hardness measurement. Nano-indentation in the continuous stiffness measurement mode was employed to characterize the hardness and elastic modulus of the films [13]. A characteristic hardness of the films was chosen as being the depth of 200 nm where the measured values were not affected by the mechanical properties of the substrate.

3. Results and discussion

Figs. 2 and 3 are the plasma shapes discharged by the 50.8 and 76.2 mm guns respectively at various working pressures of (a) 0.27 Pa, (b) 0.80 Pa, (c) 1.33 Pa and (d) 4.00 Pa. These figures show remarkable different shapes of plasma between two magnetron sputtering guns. In both figures, the discharge volume appears in the form of a brightly glowing area near the target; however, the 50.8 mm gun makes column-like plasma from the target to substrate where the deposition takes place, whereas the 76.2 mm gun makes only the hemispherical discharge with radius of 28 mm and dim plasma around the discharge. It was observed that plasma shape and brightness strongly depend on the gas pressure. Although the glowing discharge volume remains almost unchanged with the working pressure, the plasma column in Fig. 2 and dim plasma near the discharging volume in Fig. 3 is disappeared as the pressure increases.

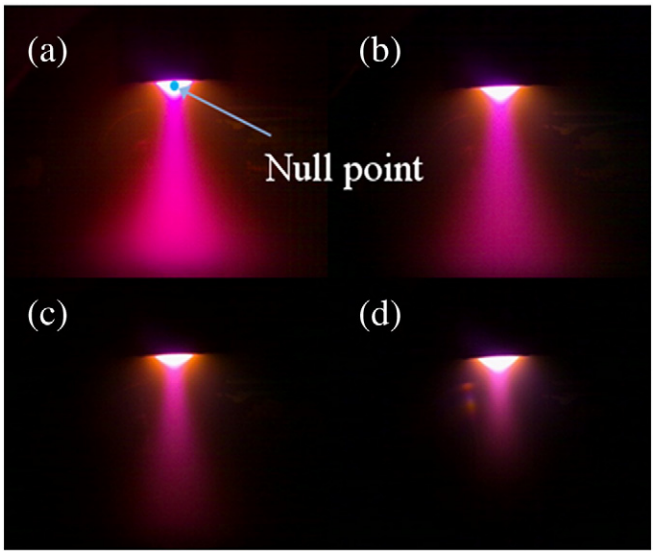

Fig. 2. Plasma shapes at the working pressures of (a) 0.27 Pa, (b) 0.80 Pa, (c) 1.33 Pa and (d) 4.00 Pa with the 50.8 mm magnetron sputtering gun.

Computer simulations have been done to clarify the cause of plasma changes with different magnetron sputtering guns. Computed magnetic field line configurations around the 50.8 and 76.2 mm guns are respectively shown in Fig. 4 (a) and (b). The magnetic field lines make a special point, a null point, where the field intensity is zero. The null point of the 50.8 mm gun is located at 27.7 mm away from the gun and the null point of the 76.2 mm gun is located at 42.4 mm away from the gun. Above the null point, most magnetic field lines come out of the side magnets and reenter the gun surface, i.e. the field lines are closed. However, below the null point, the magnetic field lines are opened toward the substrate.

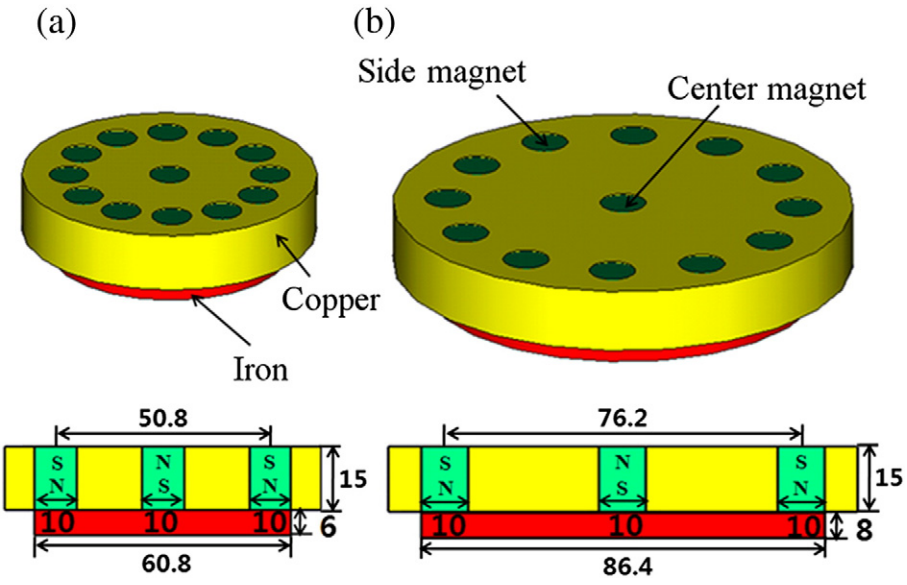

Fig. 1. Schematic diagrams of the (a) 50.8 and (b) 76.2 mm magnetron sputtering guns and their cross section views used in the experiments and simulations.

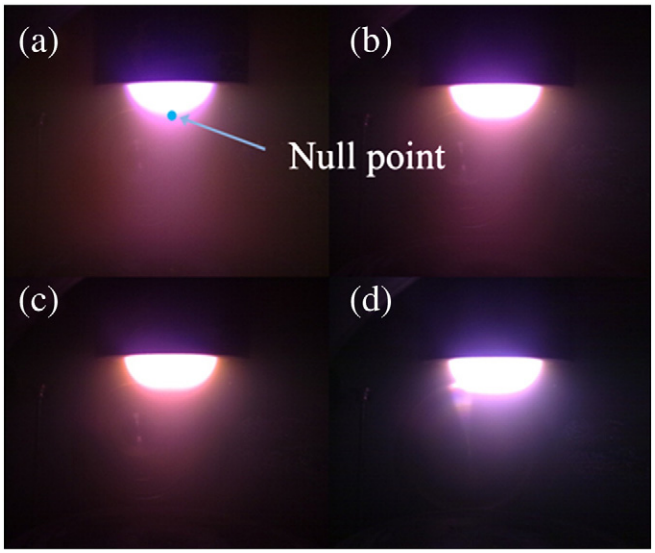

Fig. 3. Plasma shapes at the working pressures of (a) 0.27 Pa, (b) 0.80 Pa, (c) 1.33 Pa and (d) 4.00 Pa with the 76.2 mm magnetron sputtering gun.

Here we can see that there is a relationship between the position of null point and plasma shape. The glowing discharge volume is sustained by secondary electrons produced through the impact of energetic ions and a confinement of the secondary electrons by the closed-magnetic field line in the discharge volume results in a relatively high plasma density. Because the null point of the 50.8 mm gun is within the glowing discharge volume as shown in Figs. 2 (a) and 4 (a), sufficient number of secondary electrons in the discharge volume can easily move to the substrate along the magnetic field and propagate the ionization and charged particles. This movement of electrons enhances the plasma density and leads the incident ion flux with high kinetic energy to the substrate. However, the null point of the 76.2 mm gun is located at the boundary of glowing discharge volume or lower position than that. Therefore, the most charged particles are accelerated back into the plasma and are trapped near the target surface by the closed-magnetic field, ion density below the null point is very low and small ion energy and flux can reach the substrate. (Magnetic mirror force [21]). To investigate the charged particle motions under the magnetic field, the 'particle (electrons) tracking simulation' with the same condition of Fig. 4 (a) is shown in Fig. 5. 1440 electrons following Maxwell energy distribution function are evenly spread on the circular plane located 15 mm above on the null point in Fig. 5 (a) and 2.3 mm below the null point in Fig. 5 (b). As the electrons get high energy by the acceleration of the magnetic field, the lines change from blue to red. After 30 nano-seconds later, particle trajectories are differently shown as the first particle source locations. When the particle source is 15 mm above the null point of the 50.8 mm gun, only some of electrons can escape from the influence of the magnetic field and accelerate to the substrate. However, most of the particles 2.3 mm below the null points are accelerated to the substrate moving along the magnetic filed by the potential difference and the particles in Fig. 5 (b) can reach the substrate with high energy that we expected.

Another important effect of null point on the plasma behavior is the sheath lengths. Due to the null point positions, plasma bulk of the 50.8 mm gun has a shape extended from the target to the substrate and the sheath length is shorter than that of the 76.2 mm gun which has the dim plasma. When the sheath length becomes long, ions suffer more collisions as they cross the sheath and they lose their kinetic energy more. As a result, more collisions in the sheath reduce the ion

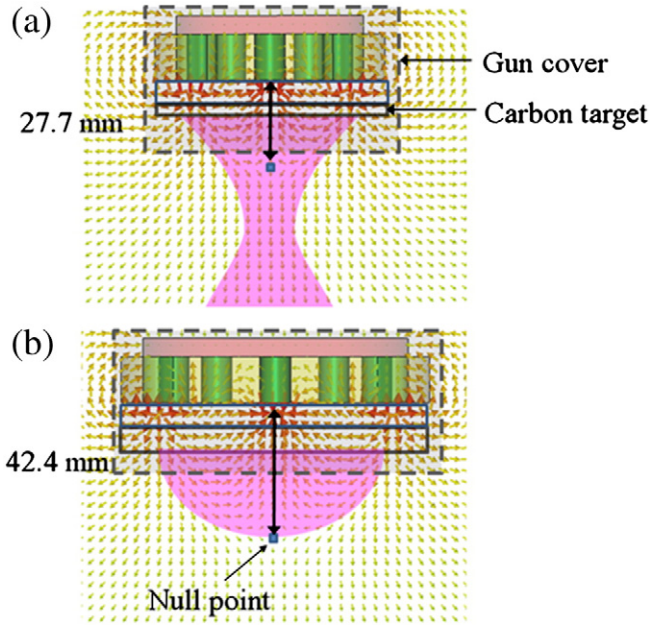

Fig. 4. Magnetic field line configurations of the (a) 50.8 and (b) 76.2 mm magnetron sputtering guns. The pink solid shapes mean the schematic figures of the plasma and discharging volume.

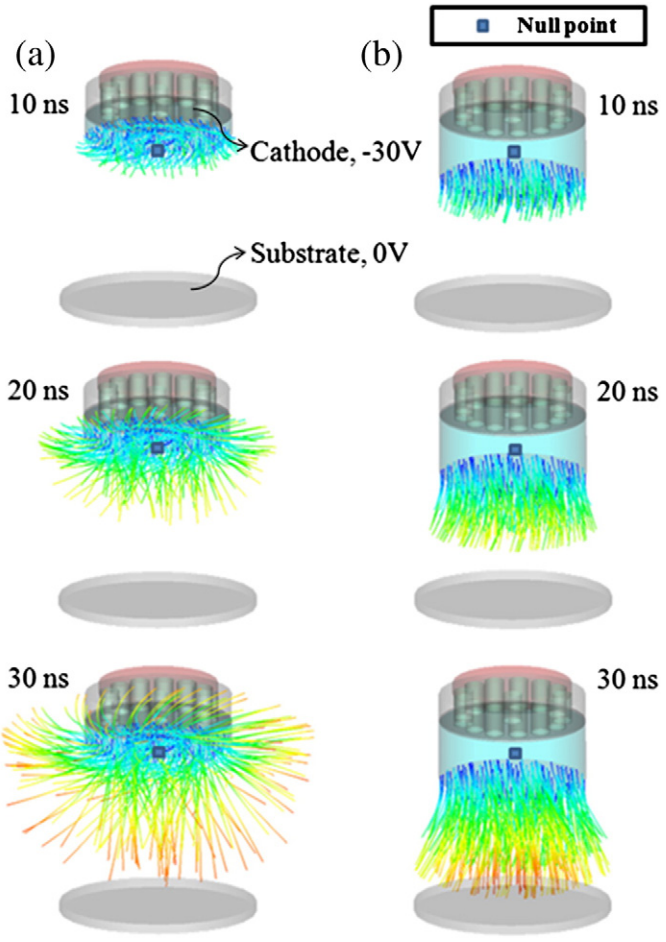

Fig. 5. Particle trajectories with different particle source locations of (a) 15 mm above the null point and (b) 2.3 mm below the null point after simulation time was changed from 10 ns to 30 ns with the 50.8 mm gun.

bombardment energy on the substrate and deposited films can have been affected by the ion energy change.

In Fig. 6, we divide the plasma of the 50.8 mm gun into two parts as 'center' and 'peripheral' regions: the high-density bright columnar plasma in the center region and the low-density dim plasma in the peripheral region. At the working pressure of 0.27 Pa, the plasma of the center region contacts with a surface of the substrate making a circle 4.5 cm in diameter. Because of the high plasma potential at low working pressure [14] and collisionless diffusion in the short sheath length, the ion bombardment energy in the center region is too high to deposit CN_x films so they would rather be resputtered than deposited. As the working pressure increases, ions in the plasma lose their kinetic energy by frequent collisions with the background gas [14]. The plasma column in the center region gradually becomes obscure and finally disappears at 4.00 Pa. Over the working pressure of 0.80 Pa, CN_x films in the center region start to be deposited on the substrate.

Fig. 7 shows the hardness of CN_x films deposited with the 50.8 and 76.2 mm guns under various working pressures. The samples are divided into three categories with the deposition conditions; CN_x films deposited on the center region with the 50.8 mm gun, CN_x films deposited on the peripheral region with the 50.8 mm gun, and CN_x films deposited with the 76.2 mm gun. Hardness of the films deposited on the peripheral region with the 50.8 mm gun and deposited on the center region with the 76.2 mm gun shows similar tendency. As the working pressure decreases from 4.00 to 0.80 Pa, the hardness of those samples slightly increases from 1.18 ± 0.04 to 1.82 ± 0.03 GPa. At 0.27 Pa of the working pressure, the hardness is abruptly increased up to 7.52 ± 0.11 GPa. On the other hand, CN_x films deposited on the center region with the 50.8 mm gun have further higher hardness than those deposited under other two conditions. The hardness of CN_x films deposited at 0.80 Pa with the 50.8 mm gun increases up to 10.3 GPa which is five times higher than that with the 76.2 mm gun.

Roh et al. [14] reported the evolution of chemical bonds in CN_x films deposited with the 76.2 mm gun as the working pressure changed and those FTIR spectra is shown in Fig. 8. The most remarkable change in the spectra is the shrinking of the absorption band at 3100–3500 cm^{-1} (which corresponds to the N–H and C–H bonds) [22,23] with decreasing gas pressure. Another main feature in Fig. 8 is that a decrease of the gas working pressure results in a decrease of the intensity of the band in the range of 1350 cm^{-1} caused by the stretching mode of the C–N single bond, and the absorption peak at approximately 1500–1600 cm^{-1} indicating absorption due to the C═N double bond [24] decreases with lower gas pressure. This result indicates that decreasing gas pressure results in an increase in the number of C–N bonds compared with that of C═N bonds.

Fig. 9 shows FTIR spectra of CN_x films deposited on the (a) peripheral and (b) center region with the 50.8 mm gun. FTIR spectra of CN_x films deposited on the peripheral region with the 50.8 mm gun are similar to those of CN_x films deposited with the 76.2 mm gun.

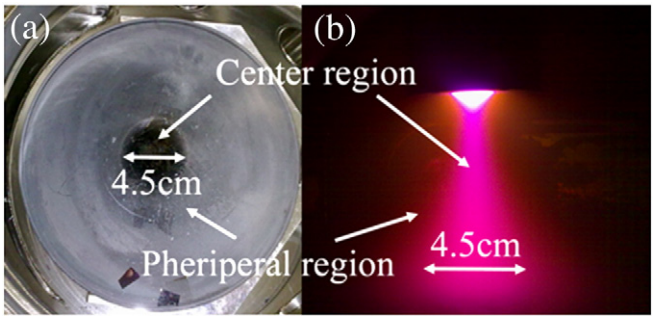

Fig. 6. Two regions of the plasma discharged by the 50.8 mm magnetron sputtering gun (a) on the substrate and (b) in the plasma volume.

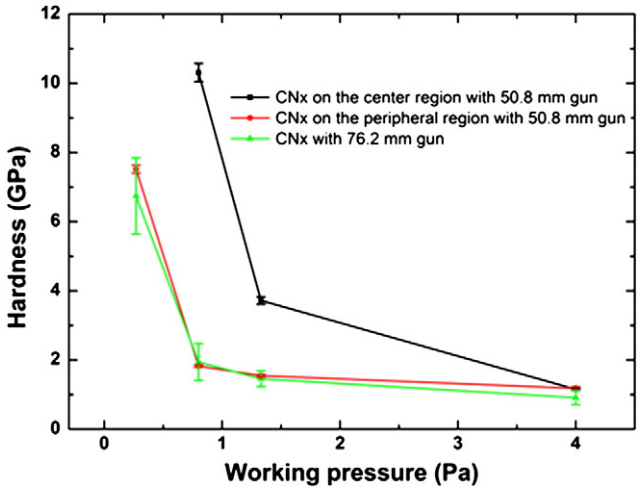

Fig. 7. Hardness of CN_x films deposited with the 50.8 and 76.2 mm guns as a function of working pressure.

However, in case of FTIR spectra of CN_x films deposited on the center region with the 50.8 mm gun, there is no peak of hydrogenated bonds at 3100–3500 cm^{-1} although the working pressure increases from 0.27 to 0.80 Pa. Besides, the peak intensity of hydrogenated bonds at 1.33 Pa is much smaller than those for other deposition conditions as shown in Figs. 8 and 9 (a). On the other hand, sp^3 C–N bond peak around 1300 cm^{-1} at 0.80 Pa is greatly bigger than even that at 0.27 Pa with the 76.2 mm gun.

The changes observed in FTIR spectra can be attributed to the fact following: for the 76.2 mm gun, most of charged particles in the discharge volume are trapped near the target surface by the magnetic field lines, therefore, the ion energy and flux on the growing film is too low to cause the weakly bonded hydrogen or hydrogen-containing species to be expelled from the film. In this case, H-terminated ions favor olefin formation, such as chains and graphite like rings having sp^2 C═N bonds and terminated by C═H or N═H than 3-dimensionally crosslink. As a result, the insufficient energetic ion bombardment changes the diamond-like micro domains to graphite-like, which results in the decrease of the hardness of CN_x films. On the other hand, for the 50.8 mm gun, because of the short sheath length and the null point within the discharge volume, the plasma can easily move and be accelerated to the substrate along the magnetic field line with

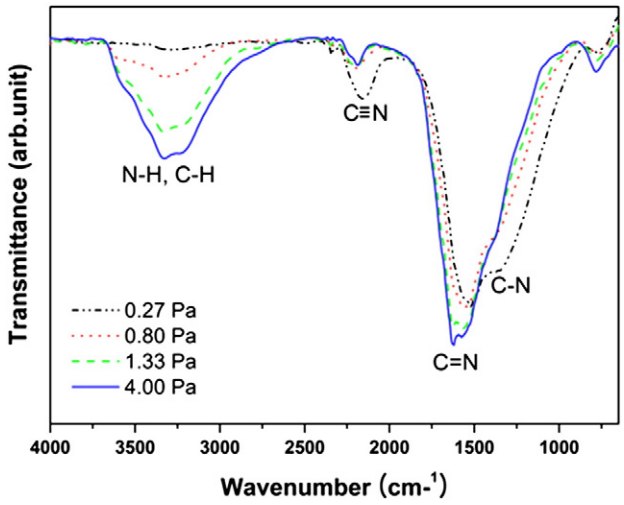

Fig. 8. FTIR spectra of CN_x films deposited at various working pressures with the 76.2 mm gun in Ref. [14].

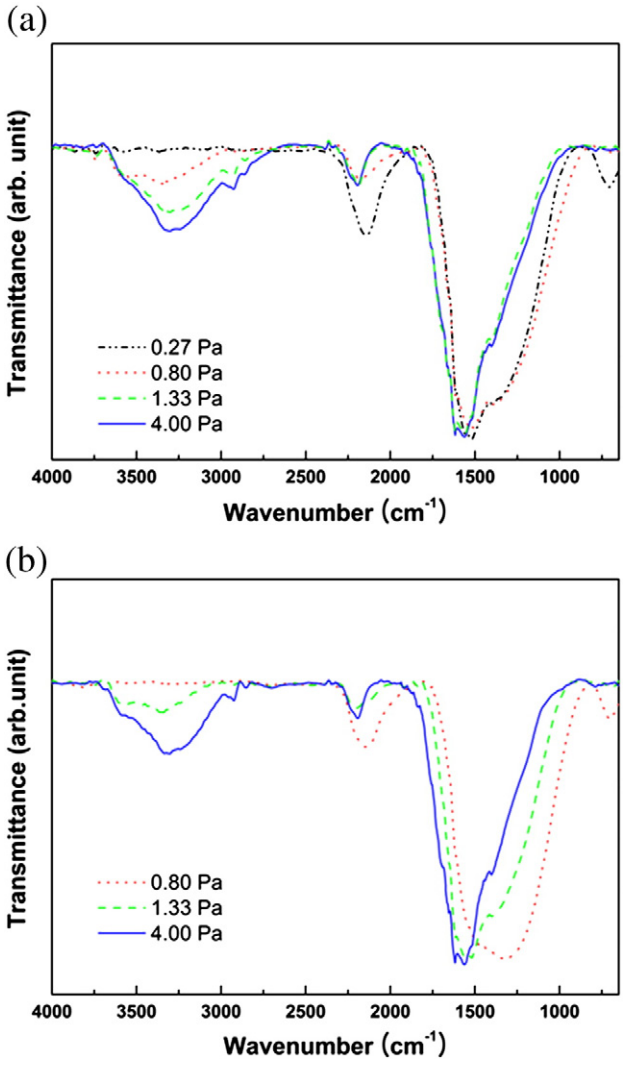

Fig. 9. FTIR spectra of CN_x films deposited on the (a) peripheral and (b) center regions at various working pressures with the 50.8 mm gun.

properly high bombardment energy so the impinging ions easily break weak hydrogenated bonds; the H-broken bonds of carbon or nitrogen atoms become favorable condition to make 3-dimensional cross-links with dangling bonds of other atoms thus CN_x films for the 50.8 mm gun have more sp^3 C – N bonds, less hydrogenated bonds and higher hardness value than those for the 76.2 mm gun deposited under the same working pressure. However, under the conditions of the 50.8 mm gun and working pressures of less than 0.80 Pa, the ion bombardment energy is too high to synthesize CN_x films so ions prefer to be resputtered than to be deposited. These results show that sufficient ion bombardment energy under the condition of low working pressure and the 50.8 mm gun contributes to synthesizing CN_x films with high hardness.

4. Conclusion

The influence of the magnetron sputtering gun size on the plasma and CN_x film properties using the 50.8 and 76.2 mm gun was investigated using CST simulation, FTIR analysis, and nano-indentation measurement. In case of using the 76.2 mm gun, the null point forms at the boundary or slightly outer than the discharge volume, so that most of charged particles in the plasma are trapped by the closed-magnetic field lines. Furthermore, when ions cross the long sheath, the number of ion collisions increases and only small ion flux with low energy can reach the substrate. On the other hand, in case of using the 50.8 mm gun, the location of the null point is within the discharge volume. The open-magnetic field lines below the null point make the charged particles in the plasma easily move and strike the substrate with properly high bombardment energy, thus the intensive ion bombardments enhance the break of weak hydrogenated bonds with ions and encourages 3-dimensional cross links in the CN_x films. As a result, the CN_x films deposited by the 50.8 mm gun contain more sp^3 C – N bonds, less hydrogenated bonds and better nano-hardness, compared with those by the 76.2 mm gun. We conclude that the gun size has strong influence on the behavior of the plasma and CN_x film deposition characteristics by changing magnetic field line configurations and positions of null points. The results of this work show that a study on the methods of changing the null point position is needed for the film deposition with modulated characteristics.

Acknowledgements

This research was supported by the Basic Research Project of the Korea Institute of Geoscience and Mineral Resources (KIGAM), which was funded by the Ministry of Knowledge Economy of Korea. This work also sponsored in part by the Korea Ministry of Knowledge Economy (10034836, 10031812-2008-11) and Korea Research Institute of Standards and Science (KRISS).

References

[1] A.Y. Liu, M.L. Cohen, Science 841 (1989) 245.
[2] W. Precht, M. Pancielejko, A. Czyzniewski, Vacuum 53 (1999) 109.
[3] H.L. Bai, E.Y. Jiang, Thin Solid Films 353 (1999) 157.
[4] C. Niu, Y.Z. Lu, C.M. Lieber, Science 261 (1993) 334.
[5] M. Kohzaki, A. Matsumuro, T. Hayashi, M. Muramatsu, K. Yamaguchi, Thin Solid Films 308 (1997) 239.
[6] T. Inoue, S. Ohshiro, H. Saitoh, K. Kamata, Appl. Phys. Lett. 67 (1995) 353.
[7] T.W. Yen, C.P. Chou, Appl. Phys. Lett. 67 (1995) 2801.
[8] S. Kundoo, A.N. Banerjee, P. Saha, K.K. Chattopadhyay, Mater. Lett. 57 (2003) 2193.
[9] H. Ito, K. Kanda, H. Saitoh, Diamond Relat. Mater. 17 (2008) 688.
[10] K. Ogata, J.F.D. Chubaci, F. Fujimoto, J. Appl. Phys. 76 (1994) 3791.
[11] J. Vlček, K. Rusňák, V. Hájek, L. Martinů, H.M. Hawthorne, Wear 213 (1997) 80.
[12] E. Broitman, N. Hellgren, K. Järrendahl, M.P. Johansson, S. Olafsson, G. Radnóczi, J.-E. Sundrren, L. Hultman, J. Appl. Phys. 89 (2001) 1184.
[13] Y.S. Park, H.S. Myung, J.G. Han, B. Hong, Thin Solid Films 475 (2005) 298.
[14] K.M. Roh, S.J. You, S.K. Choi, J.H. Kim, D.J. Seong, J. Phys. D Appl. Phys. 42 (2009) 175405.
[15] J. Vlček, K. Rusňák, V. Hájek, L. Martinů, Diamond Relat. Mater. 9 (2000) 582.
[16] R.A. Rao, Q. Gan, C.B. Eom, Y. Suzuki, A.A. McDaniel, J.W.P. Hsu, Appl. Phys. Lett. 69 (1996) 3911.
[17] M. Shao, A. Fischer, D. Grecu, U. Jayamaha, E. Bykov, G. Contreras-Puente, R.G. Bohn, A.D. Compaan, Appl. Phys. Lett. 69 (1996) 3045.
[18] H.C. Barshilia, B. Deepthia, K.S. Rajama, Vaccum 81 (2006) 479.
[19] W.D. Sproul, J. Vac. Sci. Technol. A 3 (1985) 580.
[20] http://www.cst.com.
[21] J.R. Reitz, F.J. Milford, R.W. Christy, Foundation of Electromagnetic Theory, Addison-Wesley Publishing Company, 1993, p. 349.
[22] A. de Graaf, G. Dinescu, J.L. Longueville, M.C.M. van de Sanden, D.C. Schram, E.H.A. Dekempeneer, L.J. van Ijzendoorn, Thin Solid Flms 333 (1998) 29.
[23] A. Zocco, A. Perrone, A. Luches, R. Rella, A. Klini, I. Zergioti, C. Fotakis, Thin Solid Films 349 (1999) 100.
[24] T. Szörényi, C. Fuchs, E. Fogarassy, J. Hommet, F. Le Normand, Surf. Coat. Technol. 125 (2000) 308.